Journal of Fluorescence
https://doi.org/10.1007/s10895-019-02394-0

SHORT COMMUNICATION

Analysis of Bisulfite Via a Nitro Derivative of Cyanine-3 (NCy3) in the Microfluidic Channel

Haley A. Houtwed[1] · Meng Xie[1] · Aatiya Ahmad[1] · Cody D. Masters[1] · Melissa M. Davison[1] · Kristy Kounovsky-Shafer[1] · Haishi Cao[1]

Received: 18 March 2019 / Accepted: 6 May 2019

Abstract

NCy3, a derivative of Cyanine 3 with a nitro substituent, showed a high reactivity to bisulfite in aqueous media, instantly leading to ratiometric change of absorption spectra and significant fluorescence quenching. Applied in the microfluidic channel, **NCy3** functionalize as a sensitive approach for quantitative detection of bisulfite, particularly for samples with a small volume.

Keywords Nitration · Cyanine dye · Bisulfite sensor · Microfluidic channel

Introduction

Preservative and antimicrobial reagent against oxidation and spoilage during food processing and wine fermentation [1], and is also added to dried fruit and potato products for long term storage [2]. Based on the report from the World Health Organization (WHO), the daily intake limit of sulfite is 0.7 mg/Kg [3]. High doses of sulfide shows a highly biological toxicity, causing disease and allergic reaction [4]. Recent studies reveal that bisulfite is correlated to lung cancer, cardiovascular disease and many neurological disorders [5]. However, bisulfite also exists naturally in the human body. In living cells, sulfite and bisulfite can be produced in aqueous media at physiological condition by endogenous sulfur dioxide (SO_2), which is generated from the oxidation of H_2S or sulfur containing amino acids by reactive oxygen species (ROS) [6]. Thus, the cellular level of bisulfite is able to collaterally reflect the local reducing environment in living cells [7]. Therefore, developing an efficient approach for rapid detection of sulfite is highly desired [8].

In past years, the fluorescence chemosensor has attracted a substantial amount of attention as a simple tool used to detect small molecules in vitro and in vivo due to high selectivity, sensitivity and real-time measurement [9]. Copious fluorescence approaches have been developed using different photophysical mechanisms (e.g., photoinduced electron transfer (PET), internal charge transfer (ICT), and (föster resonance energy transfer (FRET)) for quantitative measurement of various bio-important molecules [10]. However, the sensitivity and selectivity are always a challenge for fluorescence sensing approaches, particularly in biosamples [11].

Microfluidic devices offer scientists many benefits compared to larger scale systems. One benefit of using microchannels is the small volume needed to analyze a sample. Depending on the size of the channel and the number of channels, only femtoliters of the solution are required, which is cost-effective and beneficial for experiments with limited samples [12]. Additionally, microfluidics lends well to multiplexing, so a scientist can run multiple tests on a chip. Finally, microfluidics has a faster reaction time, portability, and enhanced sensitivity compared to large-scale systems [13]. Many systems already use microfluidics such as sequencing, detection of metabolites, physical DNA mapping, 3D cell culture, and optofluidics due to the aforementioned benefits [12–15].

In our group, we recently developed a reaction-based fluorescence sensor based on Cyanine 3 dye, which was able to rapidly react with HSO_3^- based on a nucleophilic addition mechanism. In the presence of HSO_3^-, **NCy3** showed a ratiometric change of absorption spectra and a strong fluorescence quenching within 3 min at 25 °C, indicating a high sensitivity and selectivity.

✉ Haishi Cao
Caoh1@unk.edu

[1] Department of Chemistry, University of Nebraska-Kearney, Kearney, NE 68849, USA

Published online: 28 May 2019

Table 1 The photophysical properties of **NCy3** [17]

Solvent	λ_{ab}(nm)	λ_{ab}(em)	$\varepsilon(cm^{-1}M^{-1})$	Φ
DMSO	578	601	27,800	0.190
Acetone	566	583	32,600	0.140
MeOH	564	581	15,200	0.148
THF	578	595	22,900	0.156
EtOAc	576	592	24,700	0.108
CH_2CI_2	567	581	34,900	0.160

NCy3 was also applied to a microfluidic device to measure the fluorescence intensity of samples with a small volume, in which a similar result was obtained, indicating **NCy3** could be used as an approach for quantitative detection of sulfite with a high affinity and selectivity in the aqueous media.

Methods

Apparatus

All reagents used for synthesis and measurements were purchased from Sigma-Aldrich (MO, USA), Fisher Scientific (USA), TCI (USA), Alfa Aesar (USA) and Acros Organics (USA) in analytical grade and were used as received, unless otherwise stated. Absorbance spectra were collected by Cary Series Uv-vis Spectrophotometer (Agilent Technologies). Fluorescence measurements were all performed by using a FluoroMax-4 Spectrofluorometer (Horiba Jobin Yvon, USA). All of fluorescence spectra were recorded in a 1 cm quartz cuvette. The excitation and emission slits were set at 2 nm. ^{1}H and ^{13}C NMR spectra were recorded on (^{1}H 300 MHz, ^{13}C 75 MHz) Bruker 300 Ultra-Shield spectrometer at room temperature. The HRMS data was collected in the Nebraska Center of Mass Spectrometry at University of Nebraska-Lincoln by using GCT Mass Spectrometer (Water, USA).

Synthesis

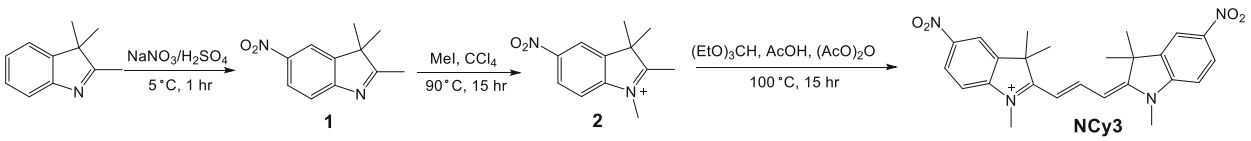

2,3,3-trimethyl-5-nitro-3H-indole (**1**). 2,3,3-trimethylindole (3.18 g, 0.02 mol) was added into concentrated H_2SO_4 (75 mL) containing HNO_3 (1.70 g, 0.02 mol) within 1 h and was incubated for 0.5 h at 0 °C [16]. After reaction, the mixture was poured into ice (1000 mL) to collect the precipatate by suction filtration. The solid was recrystallized in CH_2Cl_2 to yiled an organge ctrystall as the product (3.5 g, 91%). ^{1}H NMR (300 MHz, $CDCl_3$) δ: 1.4 (s, 6H), 2.4 (s, 3H), 7.6 (d, J = 8.3 Hz, 1H), 8.2 (s, 1H), 8.3 (d, J = 8.2 Hz, 1H). ^{13}C NMR (75 MHz, $CDCl_3$) δ: 16.1, 22.9, 54.6, 117.3, 120.3, 124.8, 145.8, 147.0, 159.3, 194.3.

1,2,3,3-tetramethyl-5-nitro-3H-indol-1-ium (**2**). A mixture of **1** (0.40 g, 0.0020 mol) and CH_3I (0.33 g, 0.0024 mol) were heated to 90 °C in CCl_4 (4 mL) for 15 h in a sealed reaction tube (50 mL). After cooling to room temperature, the reaction mixture was filtrated to yield a brown yellow solid as the pure product without any further purification (0.41 g, 95%). ^{1}H-NMR (400 MHz, $CDCl_3$) δ: 1.4 (s, 6H), 3.2 (s, 3H), 4.2 (d, J = 10.5 Hz, 2H), 6.5 (d, J = 6.7 Hz, 1H), 8.0 (s, 1H), 8.2 (d, J = 8.2 Hz, 1H). ^{13}C NMR (75 MHz, DMSO-d_6) δ: 29.4, 29.6, 43.5, 80.2, 105.5, 118.5, 126.7, 138.5, 139.6, 152.1, 161.3.

1,3,3-trimethyl-5-nitro-2-((E)-3-((E)-1,3,3-trimethyl-5-nitroindolin-2-ylidene)prop-1-en-1-yl)-5,6,7,7a-tetrahydro-3H-indol-1-ium (**NCy3**). Compound **2** (0.218 g, 0.001 mol) and triethyl orthoformate (0.593 g, 0.004 mol) were heated in acetic acid/acetic anhydride (1:1, 5 mL) at 100 °C for 12 h. After cooling to room temperature, the reaction mixture was purified by column chromatography (silica, 220–400 mesh). Ethyl acetate and methanol (4:1) were used as the elution solvents. A dard red solid (**NCy3**) was obtained as the product (0.170 g, 52%). ^{1}H-NMR (400 MHz, DMSO-D_6) δ: 1.8 (s, 12H), 3.7 (s, 6H), 6.7 (d, J = 13.5 Hz, 2H), 7.7 (d, J = 8.4 Hz, 2H), 7.7 (t, J = 5.7 Hz, 2H), 8.3–8.4 (m, 3H), 8.6 (s, 2H). ^{13}C-NMR (75 MHz, DMSO-D_6) δ: 27.4, 32.7, 49.6, 106.2, 112.6, 118.8, 126.1, 142.4, 145.0, 148.3, 152.2, 177.3. TOF EI$^+$: M^+ m/z 447.2027 (calcd.), 446.5980(found).

Microfluidic Methods

Master and Replica Fabrication

SU8 microchannel masters were fabricated by photolithography by spincoating SU8 2005 (5.0 μm, MicroChem) onto a silicon wafer and exposing it with UV-light. Replicas of the masters were created using soft lithography. PDMS (Sylgard 184) was mixed (10:1 ratio of pre-polymer to Platinum catalyst) for 15 min

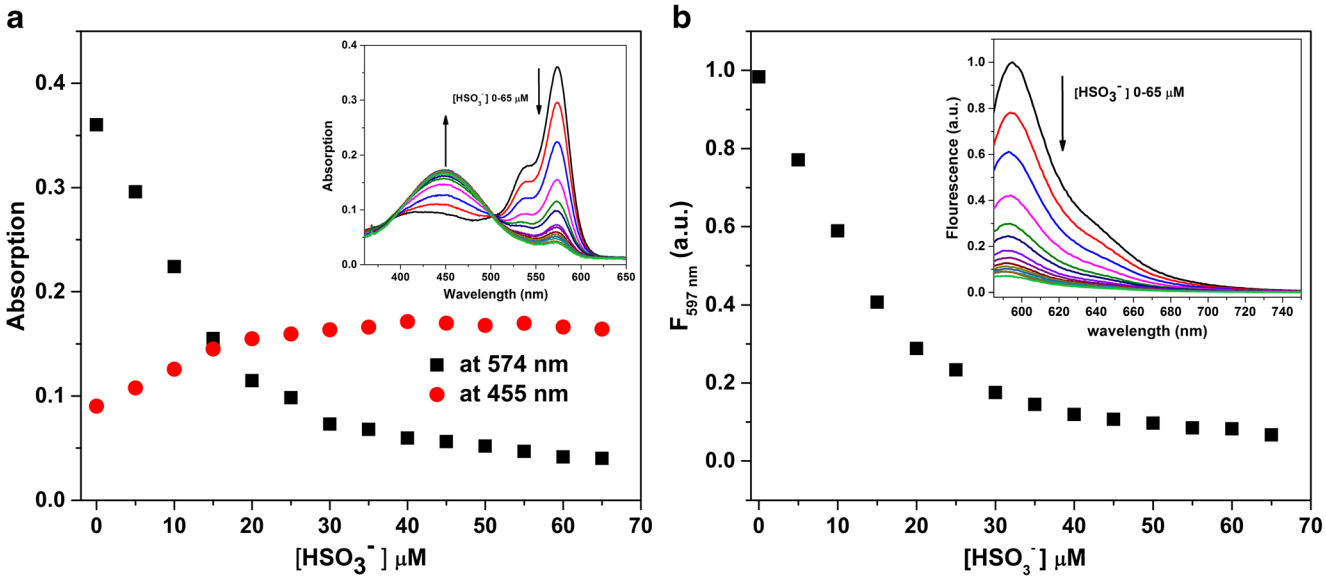

Fig. 1 The spectra change of **NCy3** (1.0×10^{-5} M) with addition of HSO_3^- (0–65 μM) in DMSO/pH 7.4 buffer (1:1) at 25 °C. **a** The absorption decreased at 574 nm and increased at 455 nm; **b** The fluorescence emission at 594 nm was gradually quenched ($\lambda_{ex} = 574$ nm)

with a hand held mixer (Kitchen Aid 9 speed mixer), poured onto the silicon master, and placed in a 65 °C oven overnight. The PDMS replica was removed from the master and then made hydrophilic with oxygen plasma treatment (Diener Zepto System, 36 s O_2 plasma, 0.50 mbar pressure, 15% power) and stored in distilled water until ready to use.

Imaging of Dye in Microchannels

The PDMS device was mounted onto coverslips and attached to a holder with candle wax. Dye (1 μL, 1×10^{-3} M) and 3 μl distilled water or 3 μl HSO_3^- (1×10^{-3} M) was mixed and loaded into microchannels via capillary action. The dynamics of the dye in the presence of water or HSO_3^- was imaged using a CoolSNAP camera and coupled to a Nikon Eclipse TE2000-S microscope. A Brightline 4040B filter set was used with X-Cite 120 Fluorescence Illumination light source to excite the dye and was captured with the NIS Elements D capture software. ImageJ was used to analyze images to compile the 2D montage and determined the fluorescence intensity for each image.[5]

Results and Discussion

The absorption and emission spectra of **NCy3** were collected in the different media, in which the maximum absorption and emission were observed in the range of 564–578 nm and 581–601 nm respectively (Table 1). **NCy3** showed the highest quantum yield (0.190) in DMSO and the lowest quantum

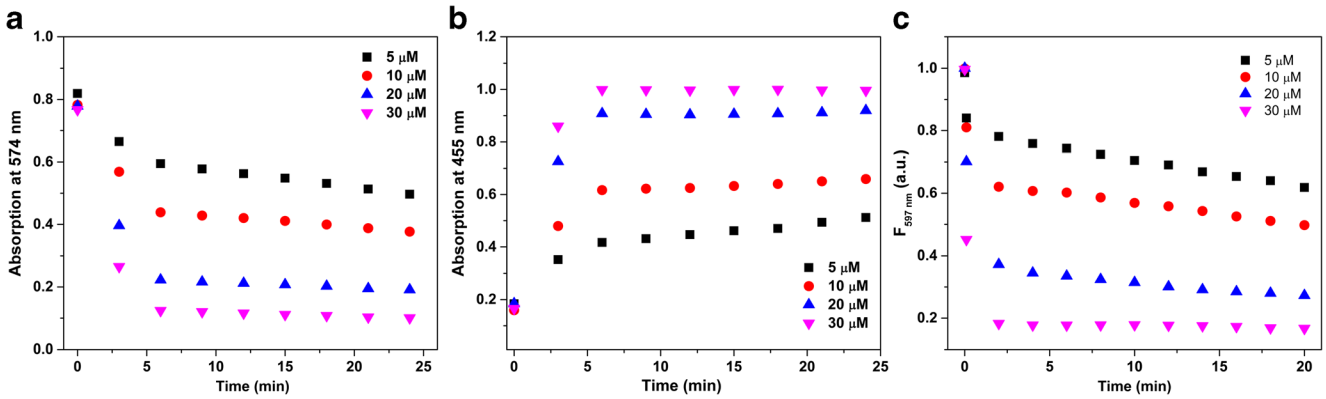

Fig. 2 The time-dependent spectrum change: (**a**) absorption at 574 nm, (**b**) absorption at 455 nm, and (**c**) emission at 594 nm of **NCy3** (1.0×10^{-5} M) with different amount of HSO_3^- (5 μM, 10 μM, 20 μM, and 30 μM) in DMSO/pH 7.4 buffer (1:1) at 25 °C

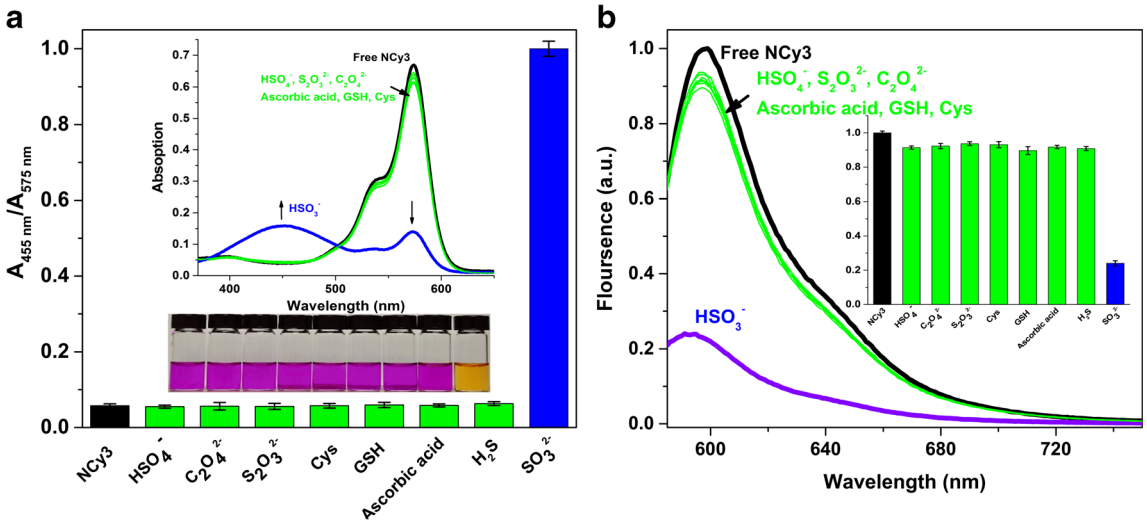

Fig. 3 The absorption responses (**a**) and fluorescence emission responses (**b**) of **NCy3** (1.0×10^{-5} M) toward HSO_4^-, $S_2O_3^{2-}$, $C_2O_4^{2-}$, Cys, GSH, ascorbic acid, H_2S and HSO_3^- (30 μM) after Incubation for 5 min in DMSO/pH 7.4 buffer (1:1) at 25 °C ($\lambda_{ex} = 574$ nm)

yield (0.108) in ethyl acetate. Based on the Consideration of solubility and photophysical properties, we chose a mixture of DMSO and H_2O (5:5, *v*/v) solution containing 20 mM phosphate buffer at pH 7.4 for **NCy3** to detect HSO_3^-.

As a nucleophile, HSO_3^- may react with **NCy3** via a nucleophilic addition reaction, which interrupts the conjugation of **NCy3** and consequently change the photophyscial properties. We first investigated the absorption and emission spectra of **NCy3** in the presence of HSO_3^- in the DMSO/buffer solution. With addition of HSO_3^- to **NCy3**, the absorption spectra rapidly showed a ratiometric signal, a dramatic decrease at 574 nm and an increase at 455 nm, indicating a significant structure change of **NCy3** (Fig. 1).

In the absorption spectra,a remarkable blue-shift (119 nm) was detected due to the interruption of π-conjugation. The instant color change, red to light yellow, was also observed by the naked eye. The maximum spectrum change was achieved when the concentration of HSO_3^- reached 30 μM, suggesting the accomplishment of the reaction. In the emission spectra, HSO_3^- led to a gradual fluorescence quench at 597 nm, and the maximum quench (92%) was observed with the addition of 30 μM HSO_3^-, which was consistent with the change of absorption spectra. The detection limit ($3\delta/k$) was calculated to be 0.086 nM based fluorescence titration at 597 nm [18].

For the reaction-based sensor, the response time is a critical factor that affects the sensing process. The chemical reaction-based signal significantly improves the sensor selectivity, but limits applications if the reaction rate is too slow. Therefore, the time-dependent spectrum change was investigated after

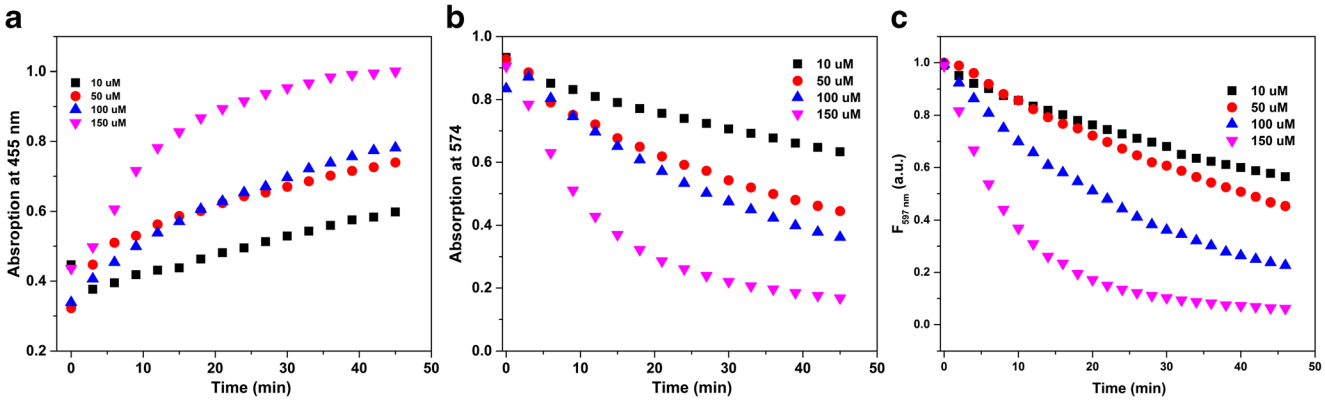

Fig. 4 The spectra change of **NCy3** (1.0×10^{-5} M) incubating with different amount of H_2S (10 μM, 50 μM, 100 μM, and 150 μM) in DMSO/pH 7.4 buffer (1:1) at 25 °C in 45 min: (**a**) the absorption change at 574 nm, (**b**) the absorption change at 455 nm, and (**c**) the fluorescence change at 594 nm ($\lambda_{ex} = 574$ nm)

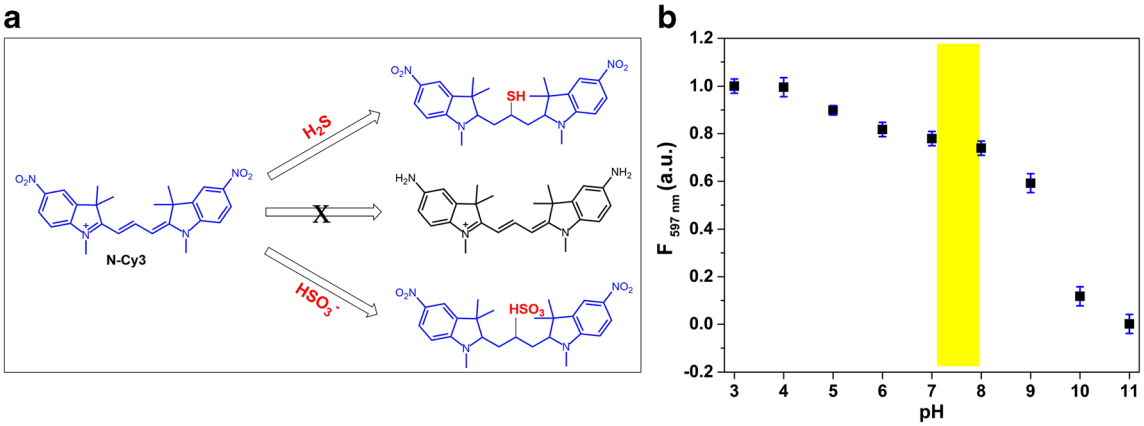

Fig. 5 **a** **NCy3** reacted with H_2S and HSO_3^- based on a nucleophilic addition mechanism. **b** The fluorescence intensity change of **NCy3** at 594 nm in different media with a pH 3.0–11.0 at 25 °C in (λ_{ex} = 574 nm)

incubation with different amount of HSO_3^- (5 μM, 10 μM, 20 μM, and 30 μM) to **NCy3** at 25 °C in the DMSO/buffer media. A change of absorption at 574 nm and 455 nm were measured as well as the emission at 597 nm. A nucleophilic reaction triggered a spectrum change instantly. After incubating HSO_3^- (5 μM) with **NCy3** at 25 °C, both absorption and emission spectra gradually changed over the course of 25 min. However, a high concentration of HSO_3^- (30 μM) led to a rapid spectra change and the maximum change was observed within 5 min, which indicated a high reaction rate based on our data for our reaction-based sensor (Fig. 2).

High affinity for a target molecule is another important factor to evaluate a sensor, and is one of the main challenges for sensor designs. To examine the selectivity of **NCy3** towards different molecules, various analytes, including biothiols, reducing reagents, and sulfur-containing ions (30 μM) were incubated with **NCy3** (1.0×10^{-5} M) for 5 min in a DMSO/Buffer media at 25 °C. Afterwards, the absorption and emission spectra were measured. As shown in the Fig. 3, all of interfering species (HSO_4^-, $S_2O_3^{2-}$, $C_2O_4^{2-}$, cysteine, glutathione, ascorbic acid, and H_2S) showed just a slight change (i.e., around 10%) in both absorption and the emission spectra. However, during incubation with HSO_3^-, **NCy3** rapidly displayed a ratiometric signal at 455 nm/575 nm in the absorption spectra as well as a significant quenching at 597 nm in the fluorescence spectra, demonstrating that **NCy3** is very sensitive to HSO_3^-, allowing **NCy3** to be used as a approach with multiple spectroscopic signal channels for rapid detection of HSO_3^-. The interruption of the conjugation of **NCy3** trigged by HSO_3^- led to an

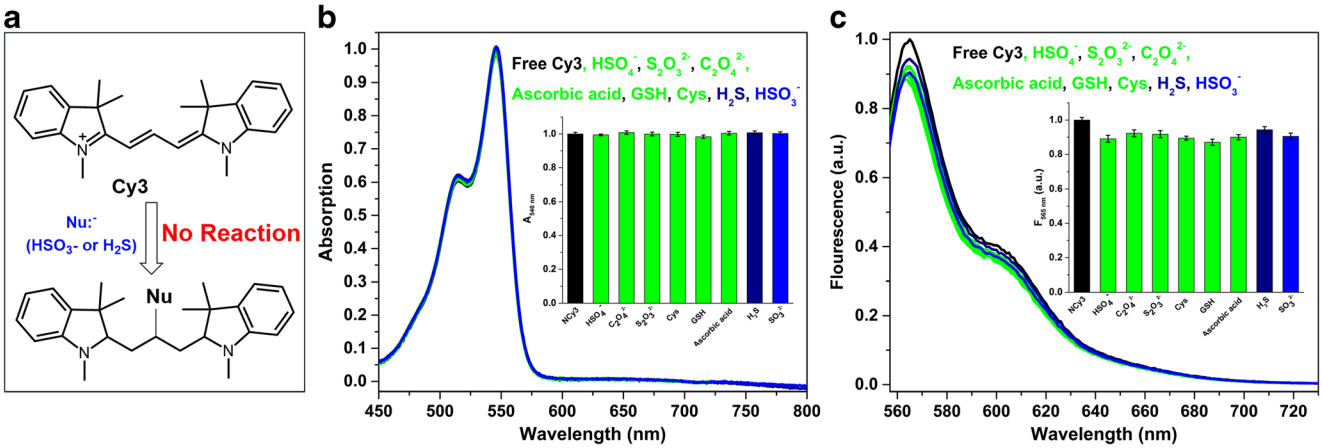

Fig. 6 After incubation **Cy3** (1.0×10^{-5} M) with HSO_4^-, $S_2O_3^{2-}$, $C_2O_4^{2-}$, Cys, GSH, ascorbic acid, H_2S and HSO_3^- (150 μM) for 30 min in DMSO/pH 7.4 buffer (1:1) at 25 °C (λ_{ex} = 574 nm), (**a**) no nucleophilic addition reaction observed; (**b**) absorption spectra and (**c**) fluorescence spectra did not show a significant change

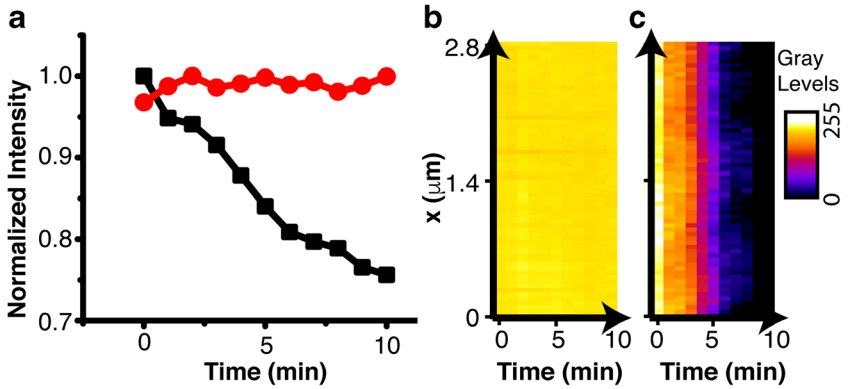

Fig. 7 **a** Intensity of the dye with water (red circles) or HSO_3^- (black squares) in 55 μm wide × 5.0 μm high microchannels was normalized and plotted against time. (B) and (C) Dynamics of the dye in the presence of water (**b**) or HSO_3^-(C) was imaged in microchannels for 10 min and compiled into a movie. A 2D slice was taken from each image at the same location and compiled to create the 2D montage (1 min per slice). The distance (x) of the slices of the image was in μm

obvious color change from light pink to yellow, which can be easily observed by naked eye, making the detection process very convenient.

As a nucleophile, H_2S did not show a high reaction rate with **NCy3** at low concentration. However, with increasing concentration and incubation time, **NCy3** gave a significant response to H_2S. As shown in the Fig. 4, both the absorption and emission spectra steadily changed within 45 min at 25 °C when the H_2S level was less than 100 μM, indicating a slow reaction process. When increasing the level of H_2S to 150 μM, the spectra displayed a relatively quick change, and plateaued after a 30-min incubation with **NCy3**, suggesting a complete reaction. Based on the previous data, **NCy3** showed a potential to detect H_2S with a high concentration. Besides H_2S, other species (HSO_4^-, $S_2O_3^{2-}$, $C_2O_4^{2-}$, Cys, GSH, and ascorbic acid) did not cause significant spectroscopic change even at high concentration and/or longer incubation time with **NCy3**.

According to previous work, the nitro group on the aromatic ring (1,8-naphthalimide) can be reduced by H_2S and consequently lead to photophysical property change, which has been intensively used as a sensing strategy for the detection of H_2S [19]. Thus, **NCy3** was incubated with different reducing reagents (H_2S, GSH, ascorbic acid, and HSO_3^-) to investigate the reduction of nitro group. However, no reduction reaction was observed in the presence of any these reducing reagents. Only HSO_3^- and H_2S led to a nucleophilic addition reaction, and HSO_3^- gave a higher reaction rate (Fig. 5a). Moreover, the pH effect in the range of pH 3–11 was examined for **NCy3** in different DMSO/buffer media. At low pH range (3.0–8.0), **NCy3** showed a strong fluorescence emission at 597 nm. With an increase of pH, the fluorescence was quenched rapidly. Although the fluorescence intensity of **NCy3** was significantly influenced by pH value, no notable change was observed in the physiological pH range (pH 7.0–8.0) (Fig. 5b).

To understand the nucleophilic addition reaction between **NCy3** and nucleophiles (e.g., HSO_3^- and H_2S), the Cyanine 3 dye (**Cy3**) without nitro groups was synthesized for a comparison. Compared to **NCy3**, **Cy3** showed a shorter absorption and emission at 546 nm and 565 nm respectively in the DMSO/pH 7.4 buffer (1:1) at 25 °C. Since **NCy3** showed a significant spectroscopic change in the presence of HSO_3^- and H_2S in high concentration, the same condition was applied to **Cy3**. However, neither absorption nor emission displayed a notable change. Moreover, high concentration (150 μM) of analytes (HSO_4^-, $S_2O_3^{2-}$, $C_2O_4^{2-}$, Cys, GSH, ascorbic acid, H_2S, and HSO_3^-) along with longer incubation time (30 min) with **Cy3** could not produce any significant spectroscopic change, revealing that no nucleophilic addition reaction occurred for **Cy3** (Fig. 6). The nucleophilic addition reaction is well established for α,β-unsaturated compounds. As an electron-withdrawing group, the nitro group on **NCy3** played a critical role in significantly boosting the addition reaction. Moreover, the HRMS data indicated that a reduction reaction followed the nucleophilic addition reaction in the present of HSO_3^-, which thoroughly explained the significant spectra change for absorption and emission.

Because **NCy3** was ultra-sensitive, ratiometric, instant, and multiple channel signal sensing abilities, **NCy3** was applied to develop a microfluidic device for analysis of HSO_3^- in very small volume samples. A PDMS device was mounted onto a coverslip and attached to a 3D printed PLA holder with candle wax [20]. Then, dye (1 μl, 1.0×10^{-3} M) and 3 μl distilled water or 3 μl HSO_3^- (1.0×10^{-3} M) was mixed and loaded into microchannels via capillary action. The dynamics of the dye in the presence of water or HSO_3^- was imaged using a CoolSNAP camera and coupled to a Nikon Eclipse TE2000-S microscope. As shown in Fig. 7, with the incubation of HSO_3^- with **NCy3** in the microchannel, a fluorescence quenching was observed within 10 min, indicating that **NCy3** was able to produce a reliable signal in a microfluidic device for detection of HSO_3^-. As a negative control, addition of H_2O did not led to a significant change in fluorescence.

Conclusions

In summary, a fluorescent probe (**NCy3**) was synthesized for detection of HSO_3^- via a nucleophilic addition reaction in aqueous media. **NCy3** demonstrated a rapid ratiometric sensing for HSO_3^- with high selectivity and sensitivity. This probe provided multiple signals, including absorption spectra, emission spectra, and colormetric signal, to quantitatively measure HSO_3^-. In addition, **NCy3** was successfully employed in developing a microfluidic device to measure trace amounts of HSO_3^- in samples with a small volume, which could be very useful for biosamples or environmental monitoring.

Acknowledgments Thanks Dr. Brandon Luedtke for help with the Nikon microscope. Financial support was provided by grants from the National Center for Research Resources (NCRR; 5P20RR016469) and the National Institute for General Medical Science (NIGMS; INBRE-8P20GM103427), a component of the National Institutes of Health (NIH) and Nebraska Research Initiative for the purchase of the Nikon microscope.

References

1. Pizzoferrato L, Di Lullo G, Quattrucci E (1998) Determination of free, bound and total sulphites in foods by indirect photometry-HPLC. Food Chem 63:275–279
2. Verma SK, Deb MK (2007) Single-drop and Nanogram level determination of sulfite (SO_3^{2-}) in alcoholic and nonalcoholic beverage samples based on diffuse reflectance Fourier transform infrared spectroscopic (DRS-FTIR) analysis on KBr matrix. J Agric Food Chem 55:8319–8324
3. Santos-Figueroa LE, Giménez C, Agostini A, Aznar E, Marcos MD, Sancenón F, Martínze-Máñez R (2013) Selective and sensitive Chromofluorogenic detection of the sulfite anion in water using hydrophobic hybrid organic–inorganic silica nanoparticles. Angew Chem Int Ed 52:13712–13716
4. Li J, Li R, Meng Z (2010) Sulfur dioxide upregulates the aortic nitric oxide pathway in rats. Eur J Pharmacol 645:143–150
5. Migliore L, Copperdè F (2009) Environmental-induced oxidative stress in neurodegenerative disorders and aging. Mutat Res 674:73–84
6. Liu Y, Li K, Wu MY, Liu YH, Xie YM, Yu XQ (2015) A mitochondria-targeted colorimetric and ratiometric fluorescent probe for biological SO_2 derivatives in living cells. Chem Commun 51:10236–10239
7. Xu W, Teoh CL, Peng J, Su D, Yuan L, Chang YT (2015) A mitochondria-targeted ratiometric fluorescent probe to monitor endogenously generated sulfur dioxide derivatives in living cells. Biomaterials 56:1–9
8. Samanta S, Halder S, Dey P, Manna U, Ramesh A, Das G (2018) A ratiometric fluorogenic probe for the real-time detection of SO_3^{2-} in aqueous medium: application in a cellulose paper based device and potential to sense SO_3^{2-} in mitochondria. Analyst 143:250–257
9. Demchenko LP (2009) Introduction to fluorescence sensing, Springer
10. Woo J, Kim G, Qintero K, Hanrahan MP, Palencia H, Cao H (2014) Investigation of desilylation in the recognition mechanism to fluoride by a 1,8-naphthalimide derivative. Org Biomol Chem 12: 8275–8279
11. Lin VS, Lippert AR, Chang CJ (2013) Cell-trappable fluorescent probes for endogenous hydrogen sulfide signaling and imaging H_2O_2-dependent H_2S production. Proc Natl Acad Sci U S A 110: 7131–7135
12. Lorena C, Palenzuela M, Pumera M (2018) (Bio)analytical chemistry enabled by 3D printing: sensors and biosensors. TrAC Trends Anal Chem 103:110–118
13. Streets AM, Zhang X, Cao C, Pang Y, Wu X, Xiong L, Yang L, Fu Y, Zhao L, Tang F, Huang Y (2014) Microfluidic single-cell whole-transcriptome sequencing. Proc Natl Acad Sci U S A 111:7048–7053
14. Gupta A, Kounovsky-Shafer KL, Ravindran P, Schwartz DC (2016) Optical mapping and nanocoding approaches to whole-genome analysis. Microfluid Nanofluid 20:44
15. Kieninger J, Weltin A, Flamm H, Urban GA (2018) Microsensor systems for cell metabolism - from 2D culture to organ-on-chip. Lab Chip 18:1274–1291
16. Noland WE, Smith LR, Rush KR (1965) Nitration of indoles. III. Polynitration of 2-alky lindoles. J Org Chem 30:3457–3469
17. Eaton DF (1988) Reference materials for fluorescence measurement. Pure Appl Chem 60:1107–1114
18. Gabriels R (1970) General method for calculating the detection limit in chemical analysis. Anal Chem 42:1439–1440
19. Kim G, Jang E, Page AM, Ding T, Carlson KA, Cao H (2016) Investigation of a sensing approach based on a rapid reduction of azide to selectively measure bioavailability of H_2S. RSC Adv 6: 95920–95924
20. Kounovsky-Shafer K, Hernández-Ortiz JP, Jo K, Odijk T, de Pablo JJ, Schwartz DC (2013) Presentation of large DNA molecules for analysis as nanoconfined dumbbells. Macromolecules 46:8356–8368